

# Compatibility and Validation of a Recent Developed Artificial Blood through the Vascular Phantom Using Doppler Ultrasound Color- and Motion-mode Techniques

Marwan Alshipli<sup>1\*</sup>, Mohannad Adel Sayah<sup>1</sup>, Ammar A. Oglat<sup>2</sup>

<sup>1</sup>Department of Radiography, Princess Aisha Bint Al-Hussein College of Nursing and Health Sciences, Al-Hussein Bin Talal University, Ma'an, Jordan,

<sup>2</sup>Department of Medical Imaging, Faculty of Applied Medical Sciences, The Hashemite University, Zarqa, Jordan

## Abstract

**Background:** Doppler technique is a technology that can raise the predictive, diagnostic, and monitoring abilities in blood flow and suitable for researchers. The application depends on Doppler shift (shift frequencies), wherein the movement of red blood cells away from the probe is determined by the decrease or increase in the ultrasound (US) frequency. **Methods:** In this experiment, the clinical US (Hitachi Avious [HI] model) system was used as a primary instrument for data acquisition and test the compatibility, efficacy, and validation of artificial blood (blood-mimicking fluid [BMF]) by color- and motion-mode. This BMF was prepared for use in the Doppler flow phantom. **Results:** The motion of BMF through the vessel-mimicking material (VMM) was parallel and the flow was laminar and in the straight form (regular flow of BMF inside the VMM). Moreover, the scale of color velocity in the normal range at that flow rate was in the normal range. **Conclusion:** The new BMF that is being valid and effective in utilizing for US *in vitro* research applications. In addition, the clinical US ([HI] model) system can be used as a suitable instrument for data acquisition and test the compatibility, efficacy, and validation at *in vitro* applications (BMF, flow phantom components).

**Keywords:** Artificial blood (blood-mimicking fluid), Doppler shift, Hitachi Avious model, *in vitro* applications, laminar flow, phantom

## INTRODUCTION

Doppler ultrasound (US) supplied an instrument which measures the blood speed and flows.<sup>[1-3]</sup> Furthermore, it utilized in the research field and clinical field investigations to quantify the range and influence of arterial disease.<sup>[4,5]</sup> In Doppler imaging of blood, the constant object is the probe, and the moving or shifting reflectors that produce the returning signal echoes are initially the blood. The Doppler frequency (Doppler-shift) is known as the variation between the frequencies of transmitted and received of US waves echoes.<sup>[6-8]</sup> The shade of gray refers to the amplitude of each speed part. The higher the amplitude, the brighter the speed shown on the screen. By agreement, the flow toward the probe is presented above the zero-speed baseline, whereas the flow far away from the scrutiny is displayed below the zero-speed baseline. Similarly, color Doppler is shown as a red color

indicated flow toward the probe, while the other blue color stated the flow far away from the scrutiny.<sup>[9-12]</sup>

Blood that precisely mimics real human blood systems in all its properties is often referred to as blood mimicking fluid (BMF). It consists of chemical fluid and powder materials are occasionally mixed to mimic physical, acoustical, and chemical properties.<sup>[13]</sup> The advantage of items used in a BMF preparation that they can construct it with general acoustic, particles, and physical properties. Furthermore, BMF is applied to compare the act of US systems for the practice of Doppler US technicians, to allow comparison of backscatter properties

**Address for correspondence:** Dr. Marwan Alshipli,

Department of Radiography, Princess Aisha Bint Al-Hussein College of Nursing and Health Sciences, Al-Hussein Bin Talal University, P.O. Box 20, Ma'an, Jordan.  
E-mail: marwanayashr@yahoo.com

Received: 30-11-2019 Revised: 27-12-2019 Accepted: 05-02-2020 Available Online: 23-04-2020

### Access this article online

Quick Response Code:



Website:  
www.jmuonline.org

DOI:  
10.4103/JMU.JMU\_116\_19

This is an open access journal, and articles are distributed under the terms of the Creative Commons Attribution-NonCommercial-ShareAlike 4.0 License, which allows others to remix, tweak, and build upon the work non-commercially, as long as appropriate credit is given and the new creations are licensed under the identical terms.

**For reprints contact:** WKHLRPMedknow\_reprints@wolterskluwer.com

**How to cite this article:** Alshipli M, Sayah MA, Oglat AA. Compatibility and validation of a recent developed artificial blood through the vascular phantom using Doppler ultrasound color- and motion-mode techniques. *J Med Ultrasound* 2020;28:219-24.

of Doppler US and to evaluate it in a Doppler flow test object or diagnostic techniques.<sup>[5,14-21]</sup>

Flow phantoms constitute a significant appliance for the development of the Doppler US mechanism for examining the blood flow. Generally, wall-less vessels are preferable to be used in preventing mismatch problems in acoustic properties between tissue-mimicking material (TMM) and the vessel wall. It allows vessel-mimicking material (VMM) to be suitable since the TMM direct link to the BMF, and reduce or remove the Doppler artifacts.<sup>[1,12,22-25]</sup>

There are two ways for color-mode (C-mode) ultrasonic imaging estimation: PW-mode (spectral Doppler) and C-flow modes. The spectral model is testing the blood speeds of arteries at a specific site. Whereas, C-flow mode utilizes C-Doppler signals overlies on a B-mode scan image of the artery to evaluate its vascularity. Both ways depend on the Doppler-shift frequencies. Thus, when the signal wave of blood cells (source) is constant, or there is no variation between transmitted and received frequencies, and in this case, the color Doppler signals undiscovered. The positive Doppler frequency occurs when the source flow approaches toward the probe, and the receiving signal frequency wave is higher than the emitting frequency. While, a negative Doppler signal frequency occurs when the blood cells move away from the probe, or in other words, when the frequency of the emitting signal is higher than returning frequency.<sup>[6,26,27]</sup>

## METHODS

### Preparation of new blood mimicking fluid

In this experiment, a BMF consisting of small particles that mimic US scatterers, such as red blood cells was used, which is essential in wall-less flow phantoms. The laboratory-made BMF was composed of scattered particles (poly [4-methyl styrene]) material of 3–8- $\mu$ m diameter mixed with distilled water (70.0%), propylene glycol PG (5.0%, Sigma-Aldrich, Germany), and polyethylene glycol PEG (25.0%, Sigma-Aldrich, Germany). Before each



**Figure 1:** Appearances of the blood-mimicking fluid sample in transparency glass

use, BMF was filtered through a paper sieve with 30  $\mu$ m pores (laboratory sieve, USM) to remove clots that could block the phantom channels. However, more details about this laboratory-made BMF were explained in the previous literature review [Figure 1].<sup>[11,12]</sup>

### Fabrication of wall-less flow phantom

The vascular wall-less flow phantom and its measurements were done and published in the previous research study.<sup>[12]</sup> The fabrication of Konjac Carrageenan (KC are two organic items that become robust and flexible form when added together in H<sub>2</sub>O), and gelatin-based TMM done.<sup>[15]</sup> In addition, the gelatin (bovine skin) helped to increase the strength of TMM. Thus, the phantom made of transparent acrylic, with the box opened from the top side of a house for the KC and gelatin-based TMM. The length, width, and height of this box are (260 mm  $\times$  120 mm  $\times$  90 mm), respectively, with plastic pipe connectors and connected to flexible tubing to a container of BMF. A hard metallic rod (8.0 mm) supplied a phantom mold for the artery (vessel) which was placed horizontally 15 mm beneath the scanning surface, because the ideal depth of real human common carotid artery (CCA) was achieved with pulsatile flow, with a depth of 15 mm, and due its significant to ensure that the relevant physical and acoustical features of this TMM which correspond to the features of real human tissues.<sup>[15]</sup> The diameter of the metal rod for the core was measured utilizing a Vernier caliper before the cooking and pouring of the TMM. To the extent that when the TMM placed in the acrylic container and then, the metallic rod immediately is removed, an artery bore is left in the TMM and allowed the BMF to pump through it. The diameter of the metallic rod determined the artery bore diameter, while the size of the container discovered the size of the phantom. The reticulated foam was used as a set factor of the TMM to the plastic pipe connectors to avoid leaking of the BMF [Figure 2].

Dynamic viscosity was measured immediately using an electronic rotational viscometer (ERV) in NOR Lab School of Physics, Universiti Sains Malaysia. The density was directly measured using DMA35 in Energy Lab School of Physics, Universiti Sains Malaysia. The speed of sound, backscattered power, and attenuation coefficient ( $\alpha$ ) were measured by applying the pulse-echo technique through the

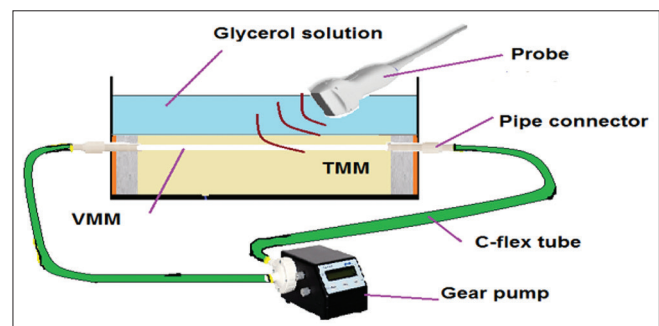


**Figure 2:** Schematic image of wall-less flow phantom, showing the use of reticulated foam to seal the channel and prevent blood-mimicking fluid leakage

ultrasonic (GAMPT) technique in Medical Physics Lab School of Physics, Universiti Sains Malaysia.

### Clinical (Hitachi Avious) ultrasound unit for data acquisition

A digital clinical US scanner (Hitachi Avious [HI]) connected with linear array transducer EUP-L74M with focal clinical frequencies ranging from 5 to 13 MHz was utilized to collect US information and data from the vascular wall-less flow phantom [Figure 3]. The probe (transducer) was placed in an adaptable probe stand and the flow phantom on a suitable flat table [Figure 4]. The probe was constant at a required angle (diagonal) and lowered near mostly to the surface of the flow phantom to prevent pressing the probe into the TMM. As the CCA tube vessel is a straight and long tube, the BMF flow direction will be linear with the CCA tube axis, parallel direction to the tube vessel wall. The angle marker that appears on the keyboard was arranged with the direction of the BMF flow. This angle is the angle between the beam produced by the US probe and the direction of BMF flow, as utilized in the US Doppler equation. The BMF velocity was measured with the HI clinical US scanner acting in PW-mode. The gate (sample) length adjusted to a suite with the entire vessel. The maximum velocity ( $V_{\max}$ ) in both the steady and pulsatile flow was measured by calculating the average maximum trace of the PW US Doppler signal utilizing HI clinical US scanner keyboard software. In addition, the resolutions (contrast, lateral, and axial) of TMM images were scanned by using Weasis Medical Viewer 1.2.7 program.

VMM diameter was measured by taking the average of several diameter measurements specified in B-mode and Doppler US via using the caliper knob. The KC with gelatin-based TMM was scanned by using the B-mode US with different frequencies. Moreover, the VMM diameter was measured before, during, and after the flow, to check the change in the TMM while applying the flow, due to its elasticity. The inlet (cross-sectional) area of the tube connected to the gear pump and the cross-sectional of the vessel was measured by utilizing the diameter measurements while applying the flow.



**Figure 3:** Hitachi Avious digital color ultrasound scanner

### Flow rate and confirming parabolic flow

The measurement values were utilized to evaluate the actual velocity (mean velocity) of the BMF flow in the vascular wall-less flow phantom by utilizing the flow rate formula<sup>[5,28]</sup> (Equation 1).

$$Q_o = A_o \times V_o \quad (1)$$

where  $Q_o$  is the flow rate volume

$$A_o \text{ is the cross-section area of the VMM} = \pi r^2 = \pi \frac{d^2}{4}$$

$d$  is the VMM diameter,  $\pi$  is constant value = 3.14, and  $V_o$  is the fluid (BMF) velocity inside the vessel.

To know the type of flow, for instance, turbulent or laminar flow, the  $R_e$  must be calculated by measuring the  $L_o$  of VMM, and it must be  $<2100$ .  $R_e$  is the Reynolds number (unitless number).

To make sure that the developed flow was done completely, the measurements were turned out far away from the vascular wall-less flow phantom entrance  $>2$  cm. The investigation was turned out to be utilizing an 8-mm diameter CCA vessel and L74M linear probe. The transducer was caught at a constant angle ( $53^\circ$ ) to the vessel, the lower gate (box) length was chosen (1.5 mm) and  $V_{\max}$  measurement was done. Note: The angle and sample length values were chosen regarding normal CCA measurements.<sup>[29-32]</sup>

The mean velocity resulted directly by HI software, and the PW spectral Doppler resulted by applying flow rate through a gear pump. This flow rate calculated by using the flow rate formula with an average of a flow velocity as an average value of normal velocity 30–45 cm/s of CCA velocity.<sup>[5]</sup> However, the Doppler box (gate) adjusted at several different depths to confirm whether the BMF behave laminar movement and the flow pattern is parabolic.



**Figure 4:** Vascular wall-less flow phantom construction using the clinical ultrasound scanner (Hitachi Avious Vision) at the Department of Medical Physics and Radiation Science, School of Physics, University of Science, Malaysia

## RESULTS AND DISCUSSION

### Pattern of scattering particles (poly [4-methyl styrene]) in the vessel mimicking material

The clotting of scattering particles (poly [4-methyl styrene]) inside the VMM was noted by motion-mode (M-mode) scan [Figure 5] after resting the fluid for a long time (more than 7 weeks) without pumping throughout. As can be seen in Figure 6, there was no clotting for 3 weeks, because of the powder material combined during this time (after 7 weeks). In other words, the clotting of scattering particles of BMF will also be inside the vessel.

When the BMF stirred (pumping) again for at least one or 2 h, the clotting was reduced and then disappeared. Thus, stirring the BMF before using it is a very important factor. This principle mimics the real blood because if real blood stop of flow, the clotting of the red cell will occur then many of the diseases result, while the clotting of the BMF (*in vitro*) causes TMM rupture and leakage of blood. Furthermore, the BMF produced in this research mimic the commercial BMF, which clots after resting for a long time, and the clotting was reduced and disappeared after stirred it again.

The scattering particles of BMF (poly [4-methyl styrene]) do not cause any clotting during both steady and pulsatile flow at a different flow rate and with long-term (several weeks of flow). Moreover, it does not cause any obstruction, but it was mimic the previous commercial scatters particles used in BMF since both BMF were clotted and aggregated after resting the fluid for a long time without utilizing [Figure 5].

Moreover, the results found that the BMF should keep it outside the vessel phantom and should not stay in the vessel phantom when it is not in use because the particles that used in BMF cause clotting and settling when not being used. Then, the clotting leads to obstruction (TMM rupture) and affects the vessel size when used in future.

### Circulation pattern of blood mimicking fluid inside the vessel mimicking material

The motion process in the VMM is very important to check the changes in the manifestation of motion goals of VMM since it affects the accuracy of diagnosis. Figure 7 displays the flow pattern of BMF, which was scanned by M-mode with a color image. The circulation of BMF inside the VMM was normal for several reasons. The image ensured that the motion of BMF through the VMM is parallel and the flow is laminar and in a straight form (regular flow of BMF inside the VMM). The flow was parallel and laminar because there was no spike artifact of BMF through the VMM since it was degassing well by a vacuum pump and since its backscatter power was suitable and mimic to the real human blood. Furthermore, because the wall of VMM was constant, strong, and there was no leakage of TMM. Moreover, ultimately, the Reynolds Number  $R_c$  number was  $<2100$ .<sup>[5]</sup>

First, the flow is in the direction of BMF inside the vessel, and it was forward (antegrade) not backward. In other words, if the flow direction is backward, it means that the gear motor pump

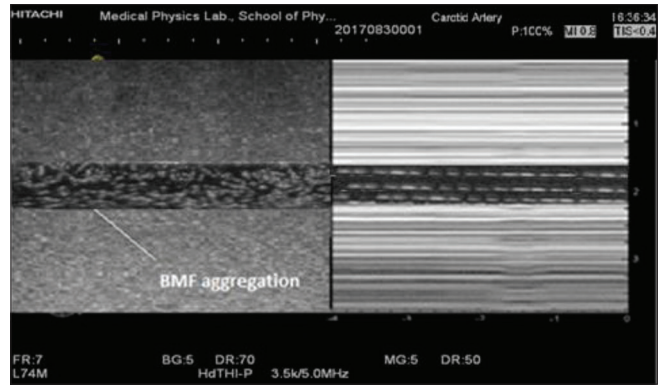


Figure 5: A gray-scale image of a longitudinal and M-mode image display showing the clotting of the BMM inside the VMM without stirred (pumping) it



Figure 6: Appearances of the blood mimicking fluid sample in transparency glass. (a) After 3 weeks (1–6 weeks). A precipitate or float did not appear, and the acoustical properties didn't change. (b) After 7 weeks. The poly (4-methyl styrene) particles were started clotting, but precipitate or float did not appear too. Liquid density: 1.04 g/ml. Particle diameter: 3–8  $\mu\text{m}$

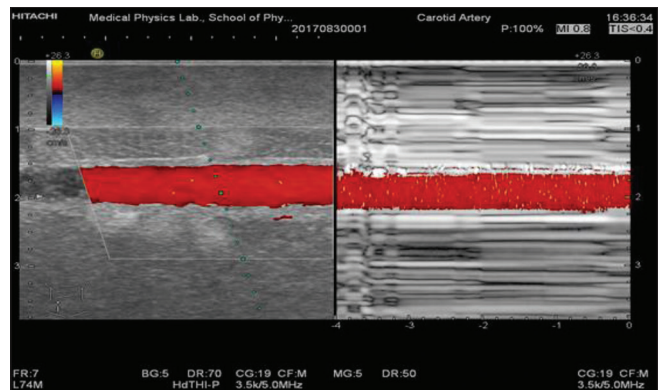
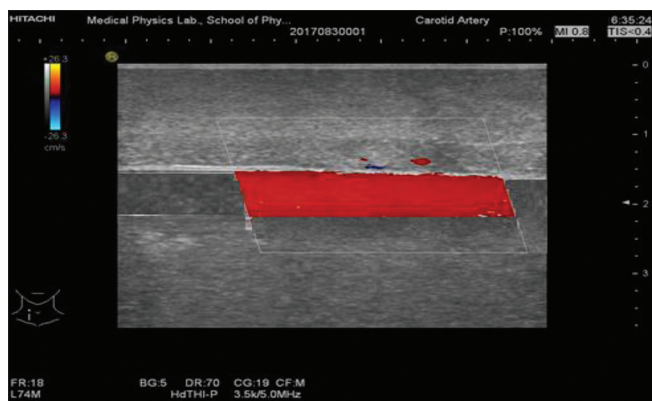


Figure 7: Longitudinal color and motion Doppler image showing a color Doppler map of mean velocity

does not work correctly or there is obstruction of TMM and VMM. Second, the blood flow during the VMM was red, not blue (BMF flow against the beam direction) since the beamline toward the flow.



**Figure 8:** Longitudinal color Doppler image shows a color Doppler map of mean velocity for normal, parallel, and laminar flow of blood-mimicking fluid in the vessel

### Color flow velocity measurements

Figure 8 shows the scale of color velocity which was resulted and adjusted at a range of  $\pm 26.3$  cm/s, this is mean that it is in normal range at this flow rate (1125 ml/min), and this indicated that the flow rate applied is true (normal) and the motor pump was worked properly. However, in real CCA, the scale of color velocity must be in a range of 25–40 cm/s as a normal range to prevent miss of the aliasing artifact when the scale of color velocity is up to the normal range 25–40 cm/s.<sup>[33]</sup>

Furthermore, Figure 8 shows that there was no aliasing artifact because when the color velocity scale is adjusted below the level of the mean velocity ( $V_m < 25$  cm/s) of the blood flow, the aliasing artifact during the artery vessel lumen will appear.<sup>[32]</sup> Moreover, there was no rupture of TMM or spike of BMF, because if there were like those obstructions, the color velocity scale would have adjusted sufficiently higher than the  $V_m$  of blood flow ( $>40$  cm/s). In contrast, when the color velocity scale is adequately adjusted higher than the  $V_m$  of blood flow, the aliasing artifact will disappear, but the stenosis and other obstructions missed.

As can be seen in Figures 7 and 8, the positive scale of color velocity (BMF inside the VMM was with normal color and with normal color speed scale appearance) resulted because the receiving signal frequency wave was higher than the emitting frequency and this indicates to the appropriate of scattering particles during flow. Furthermore, the result of normal color speed scale appearance, because when the low color speed scale is applied, the image frame rate may look like slow and haze (unclear).<sup>[34,35]</sup>

### CONCLUSION

It can be concluded that all US diagnostic parameters (B-mode, M-mode, and C-mode) in the vascular wall-less flow phantom was carried out, and its values were close within a normal range of CCA. Moreover, the BMF and flow phantom were valid in utilizing for B-mode and Doppler diagnostic *in vitro* research applications. In addition, the clinical US ([HI] model)

system can be used as a suitable instrument for data acquisition and test the compatibility, efficacy, and validation at *in vitro* applications (BMF, TMM, and VMM).

### Acknowledgment

We want to thank Department of Medical Imaging, Faculty of Applied Medical Sciences, The Hashemite University, Zarqa, Jordan for their good efforts to Pattyn G. Creating *in-vitro* hantoms of blood vessels to support the testing and validation of new ultrasonic blood flow imaging techniques. 2016;23 (4), 1.ake this work brilliant.

### Financial support and sponsorship

This research study was supported by Universiti Sains Malaysia, Medical Physics and Radiation Science Department.

### Conflicts of interest

There are no conflicts of interest.

### REFERENCES

- Grand-Perret V, Jacquet JR, Leguenerny I, Benatsou B, Grégoire JM, Willoquet G, et al. A Novel microflow phantom dedicated to ultrasound microvascular measurements. *Ultrason Imaging* 2018;40:325-38.
- Oglat AA, Matjafri MZ, Suardi N, Oqlat MA, Abdelrahman MA, Oqlat AA. A Review of Medical Doppler ultrasonography of blood flow in general and especially in common carotid artery. *J Med Ultrasound* 2018;26:3-13.
- Oglat AA, Matjafri MZ, Suardi N, Oqlat MA, Abdelrahman MA, Oqlat AA, et al. Chemical Items used for preparing tissue-mimicking material of wall-less flow phantom for Doppler ultrasound imaging. *J Med Ultrasound* 2018;26:123-7.
- Auboire L, Escoffre JM, Fouan D, Jacquet JR, Ossant F, Grégoire JM, et al. Evaluation of high resolution ultrasound as a tool for assessing the 3D volume of blood clots during *in vitro* thrombolysis. *Sci Rep* 2017;7:6211.
- Kenwright DA, Laverick N, Anderson T, Moran CM, Hoskins PR. Wall-less flow phantom for high-frequency ultrasound applications. *Ultrasound Med Biol* 2015;41:890-7.
- Ferreira JC, Ignácio FS, Meira CD. Doppler ultrasonography principles and methods of evaluation of the reproductive tract in mares. *Acta Scientiae Veterinariae* 2011;39 (Suppl. 1).
- Mehra S. Role of duplex Doppler sonography in arterial stenoses. *J Indian Acad Clin Med* 2010;11:294-99.
- Hangiandreou NJ. AAPM/RSNA physics tutorial for residents. Topics in US: B-mode US: Basic concepts and new technology. *Radiographics* 2003;23:1019-33.
- Wood MM, Romine LE, Lee YK, Richman KM, O'Boyle MK, Paz DA, et al. Spectral Doppler signature waveforms in ultrasonography: A review of normal and abnormal waveforms. *Ultrasound Q* 2010;26:83-99.
- Oglat AA, Matjafri MZ, Suardi N, Abdelrahman MA, Oqlat MA, Oqlat AA. A New Scatter particle and mixture fluid for preparing blood mimicking fluid for wall-less flow phantom. *J Med Ultrasound* 2018;26:134-42.
- Oglat AA, Matjafri MZ, Suardi N, Abdelrahman MA, Oqlat MA, Oqlat AA. A new scatter particle and mixture fluid for preparing blood mimicking fluid for wall-less flow phantom. *Journal of medical ultrasound* 2018;26:134.
- Oglat AA, Matjafri MZ, Suardi N, Oqlat MA, Oqlat AA, Abdelrahman MA, et al. Characterization and Construction of a Robust and Elastic Wall-Less Flow Phantom for High Pressure Flow Rate Using Doppler Ultrasound Applications. *Natural and Engineering Sciences* 2018;3:359-77.
- Oglat AA, Suardi N, Matjafri MZ, Oqlat MA, Abdelrahman MA, Oqlat AA. A review of suspension-scattered particles used in blood-mimicking fluid for Doppler ultrasound imaging. *J Med Ultrasound* 2018;26:68-76.

14. Ramnarine KV, Nassiri DK, Hoskins PR, Lubbers J. Validation of a new blood-mimicking fluid for use in Doppler flow test objects. *Ultrasound Med Biol* 1998;24:451-9.
15. Zhou X, Kenwright DA, Wang S, Hossack JA, Hoskins PR. Fabrication of Two Flow Phantoms for Doppler ultrasound imaging. *IEEE Trans Ultrason Ferroelectr Freq Control* 2017;64:53-65.
16. Thorne ML, Poepping TL, Rankin RN, Steinman DA, Holdsworth DW. Use of an ultrasound blood-mimicking fluid for Doppler investigations of turbulence *in vitro*. *Ultrasound Med Biol* 2008;34:1163-73.
17. Oates CP. Towards an ideal blood analogue for Doppler ultrasound phantoms. *Phys Med Biol* 1991;36:1433-42.
18. Yoshida T, Tanaka K, Sato K, Kondo T, Yasukawa K, Miyamoto N, *et al.* Blood-mimicking fluid for the Doppler test objects of medical diagnostic instruments. In 2012 IEEE International Ultrasonics Symposium. IEEE; 2012. p. 1-4.
19. Yoshida T, Sato K, Kondo T. Blood-mimicking fluid using glycols aqueous solution and their physical properties. *Jpn J Appl Phys* 2014;53 (7 Suppl):1-4.
20. Oglat AA, Matjafri MZ, Suardi N, Abdelrahman MA, Oqlat MA, Oqlat AA, *et al.* Acoustical and Physical Characteristic of a New Blood Mimicking Fluid Phantom. In *Journal of Physics: Conference Series*. IOP Publishing; 2018;1083:012010.
21. Oglat AA, Matjafri MZ, Suardi N, Oqlat MA, Abdelrahman MA, Oqlat AA, *et al.* Measuring The Acoustical Properties of Fluids and Solid Materials Via Dealing With A-SCAN (GAMPT) Ultrasonic. In *Journal of Physics: Conference Series*. IOP Publishing; 2018;1083:012053.
22. Browne JE. A review of Doppler ultrasound quality assurance protocols and test devices. *Phys Med* 2014;30:742-51.
23. Meagher S, Poepping TL, Ramnarine KV, Black RA, Hoskins PR. Anatomical flow phantoms of the nonplanar carotid bifurcation, Part II: experimental validation with Doppler ultrasound. *Ultrasound Med Biol* 2007;33:303-10.
24. Ramnarine KV, Anderson T, Hoskins PR. Construction and geometric stability of physiological flow rate wall-less stenosis phantoms. *Ultrasound Med Biol* 2001;27:245-50.
25. Rickey DW, Picot PA, Christopher DA, Fenster A. A wall-less vessel phantom for Doppler ultrasound studies. *Ultrasound Med Biol* 1995;21:1163-76.
26. Sound SO. Physics and instrumentation in Doppler and B-mode ultrasonography. *Introduction Vasc Ultrason E-Book* 2012;1550:20.
27. Ginther O, Utt MD. Doppler ultrasound in equine reproduction: Principles, techniques, and potential. *J Equine Vet Sci* 2004;24:516-26.
28. Maulik D, Zalud I. (Eds.). *Doppler ultrasound in obstetrics and gynecology*. Berlin Heidelberg New York: Springer; 2005. p. 363-74.
29. Douville Y, Johnston KW, Kassam M, Zuech P, Cobbold RS, Jares A. An *in vitro* model and its application for the study of carotid Doppler spectral broadening. *Ultrasound Med Biol* 1983;9:347-56.
30. McNaughton DA, Abu-Yousef MM. Doppler US of the liver made simple. *Radiographics* 2011;31:161-88.
31. Hoskins PR. Ultrasound techniques for measurement of blood flow and tissue motion. *Biorheology* 2002;39:451-9.
32. Lee W. General principles of carotid Doppler ultrasonography. *Ultrasonography* 2014;33:11-7.
33. Tahmasebpour HR, Buckley AR, Cooperberg PL, Fix CH. Sonographic examination of the carotid arteries. *Radiographics* 2005;25:1561-75.
34. Bluth EI, Stavros AT, Marich KW, Wetzner SM, Auffrichtig D, Baker JD. Carotid duplex sonography: A multicenter recommendation for standardized imaging and Doppler criteria. *Radiographics* 1988;8:487-506.
35. Nelson TR, Pretorius DH. The Doppler signal: Where does it come from and what does it mean? *AJR Am J Roentgenol* 1988;151:439-47.